

# PREDICTIVE DESIGN AND INTERPRETATION OF COLLIDING PULSE INJECTED LASER WAKEFIELD EXPERIMENTS\*

E. Cormier-Michel<sup>†</sup>, V.H. Ranjbar, B. Cowan, D.L. Bruhwiler, Tech-X Corporation, Boulder, CO, USA  
 M. Chen, C.G.R. Geddes, E. Esarey, C.B. Schroeder, W.P. Leemans, LBNL, Berkeley, CA, USA

## Abstract

The use of colliding laser pulses to control the injection of plasma electrons into the plasma wake of a laser-plasma accelerator is a promising approach to obtain reproducible and tunable electron bunches with low energy spread and emittance. We present recent particle-in-cell simulations of colliding pulse injection for parameters relevant to ongoing experiments at LBNL. We perform parameter scans in order to determine the best conditions for the production of high quality electron bunches, and compare the results with experimental data. We also evaluate the effect of laser focusing in the plasma channel and of higher order laser mode components on the bunch properties.

## INTRODUCTION

With accelerating gradients three orders of magnitude higher than conventional accelerators, laser-plasma based accelerators (LPA) can reduce considerably the distance needed to bring particles to high energy [1]. Recently, mono-energetic electron beams have been produced at the 100 MeV level in only 2 mm [2] and at 1 GeV in 3 cm [3] using this method. Controlled injection of high quality beams is necessary for applications such as high energy colliders [4] or Thomson gamma sources [5]. In LPAs, this can be achieved through injection from plasma density gradients [6], ionization of high  $Z$  atoms present in the plasma [7] or via colliding laser pulses (CPI) [8].

In the CPI method electrons of the background plasma are trapped in a slow beat wave produced by the interaction of two counter-propagating laser pulses and pushed on the trapped orbits of the wakefield driven by an intense laser pulse [9, 10, 11]. Current experiments use two laser pulses where the driver pulse also interacts with a lower intensity counter-propagating pulse to trap and accelerate electrons. This method produces reproducible, tunable electron beams with low energy spread and emittance [12].

In this paper, we present self-consistent particle-in-cell (PIC) simulations, using the VORPAL framework [13], of the CPI mechanism, with parameters relevant to LOASIS experiments at LBNL [14]. Laser and plasma parameters

\* Work supported by the Department of Energy, Office of National Nuclear Security Administration, NA-22, and Office of Science, Office of High Energy Physics under contract No. DE-AC02-05CH11231, and via the ComPASS SciDAC project, grant No. DE-FC02-07ER41499, and by Tech-X Corporation. This work used resources of NERSC, which is supported by the Office of Science of the U.S. Department of Energy under Contract No. DE-AC02-05CH11231.

<sup>†</sup> ecormier@txcorp.com

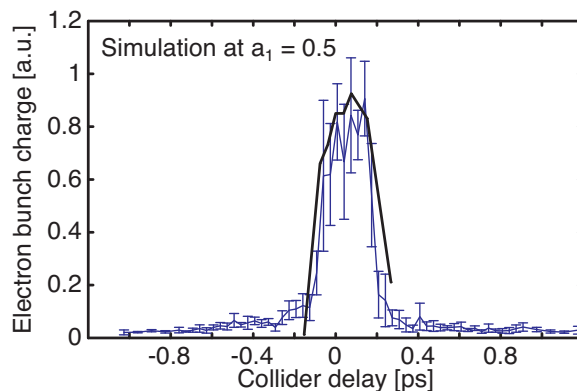


Figure 1: Trapped charge versus delay between the two laser pulses, for simulations (black) and experiment (blue).

are varied to determine the conditions for the production of the best quality electron beams as well as to establish parameters for the tunability of the beam. In addition, self-consistent simulations allow access to the internal dynamics, which helps optimize injection results. Here we present parameter scans that were used to guide CPI experiments at LBNL. We also comment on the effects of laser focusing in a plasma channel and presence of higher order laser modes in the driver pulse on the quality of the electron bunch.

## PARAMETER SCANS

Parameter ranges are chosen to be relevant to ongoing experiments at LBNL, using the 10 TW laser system of LOASIS laboratory. The main laser used to drive the wake is 0.6 J with a spot size  $w_0 \simeq 6 \mu\text{m}$  and  $a_0 \simeq 2$ , with  $a_0 \simeq 0.85 \times 10^{-9} \lambda [\mu\text{m}] (I [\text{W}/\text{cm}^2])^{1/2}$ , where  $\lambda$  is the laser wavelength and  $I$  the laser intensity. The collider laser is  $\simeq 0.25$  J, with a duration of 50 to 100 fs, a spot size  $w_1 \simeq 10 \mu\text{m}$  and an intensity  $a_1 \simeq 0.1 - 1$ . The two lasers collide with a  $19^\circ$  angle in a plasma of density which can be varied up to  $n_0 = 3 \times 10^{19} \text{cm}^{-3}$  in the experiments [14]. In the following we refer to the laser parameters such that the normalized potential is of the form  $a = a_{0,1} \exp(-x^2/L_{0,1}^2) \exp(-r^2/w_{0,1}^2)$  with  $L_{0,1}$  the pulse length and  $w_{0,1}$  the spot size, the indices (0, 1) referring to the laser driver and collider, respectively.

Even though the wake is driven in a highly non-linear regime, the trapping threshold is too low for any trapping to occur with only the main laser pulse. The trapping is turned on when the two laser overlap within a delay of  $\pm 200$  fs, for  $a_1 = 0.5$ ,  $L_0 = 11.5 \mu\text{m}$ ,  $L_1 = 18 \mu\text{m}$ ,

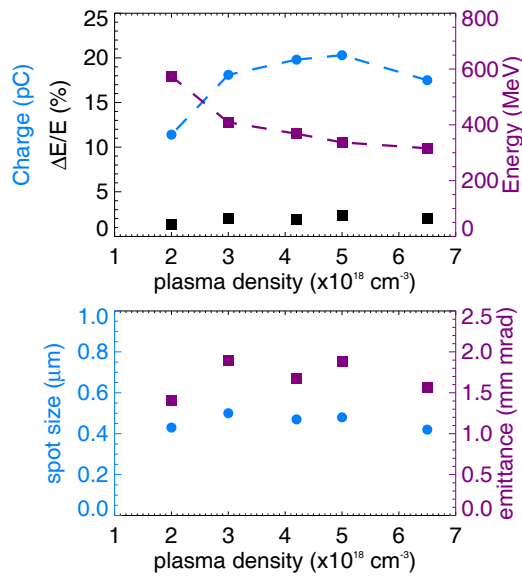


Figure 2: Trapped electron beam properties as a function of plasma density.

$n_0 = 4.2 \times 10^{18} \text{ cm}^{-3}$  and with other parameters as mentioned above. The trapped charge stays constant, with  $\sim 20\%$  variation, within the central 200 fs. This is confirmed in the experiments as seen on Fig. 1, where trapped charge as a function of delay between the two pulses is plotted for both experimental and simulation data.

The amount of trapped charge can be controlled by changing the plasma density. For these laser parameters simulations show an optimum for the trapped charge around  $n_0 \sim 3 \times 10^{18} \text{ cm}^{-3}$ . Experiments observe a similar optimum at  $n_0 \sim 4 \times 10^{18} \text{ cm}^{-3}$ , although with a shorter laser driver, consistent with the higher optimal density [14]. Because the interaction volume stays constant, decreasing the plasma density decreases the number of electrons available for trapping, leading to less trapped charge. On the other hand, by increasing the density the resonant condition  $L_0 \sim \lambda_p$ , with  $\lambda_p = (\pi m c^2 / n_0 e^2)^{1/2}$  the plasma wavelength, is no longer satisfied and the wakefield amplitude decreases, increasing the trapping threshold. That is, it requires a larger kick to the particles to be pushed from the cold fluid orbit on the trapped orbit of the main wake.

A density scan around the density optimum, with a plasma channel, reveals that there is a range in density where the trapped charge remains constant. The presence of the plasma channel allows for higher energy gain of the electron beam as the laser does not diffract and maintains high intensity over the whole acceleration length, keeping the accelerating field strength high. As seen in Fig. 2, all beam parameters remain the same between  $n_0 \simeq 3 \times 10^{18} \text{ cm}^{-3}$  and  $n_0 \simeq 6 \times 10^{18} \text{ cm}^{-3}$ , except for the final energy of the beam which varies because of the change of dephasing length. Hence for a certain density range, it is possible to tune independently the final energy of the electron beam.

On the other hand, when scaling the laser parameters

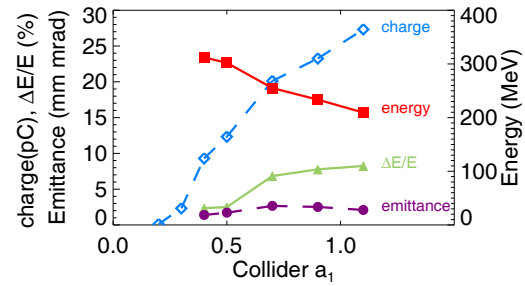


Figure 3: Trapped electron beam properties as a function of collider intensity.

with the plasma density, i.e., all lengths are varied proportionally with the plasma wavelength, the beam parameters follow the scaling laws predicted by the linear theory. The dephasing length varies as  $1/n_0^{3/2}$ , the energy gain varies as  $1/n_0$ , and the trapped charge varies as  $1/n_0^{1/2}$ , which corresponds to the scaling giving the same amount of beam loading for all densities [1, 15], while beam emittance and energy spread stay constant. Using the linear scaling laws can allow for a quick design of the accelerator properties, i.e., while the parameters used in current experiments could produce  $\sim 20$  pC beams at 300 MeV with few percent energy spread, 1.4 J driver and 0.5 J collider lasers are necessary to produce  $\sim 40$  pC beams at 1 GeV with a plasma density  $n_0 = 10^{18} \text{ cm}^{-3}$ .

The charge of the beam can also be controlled by varying the product of the two laser intensities  $a_0 a_1$  [8, 9]. This is shown in Fig. 3 where the intensity of the collider pulse,  $a_1$ , is varied. The same behavior is observed as in the experiment where charge starts to be trapped at  $a_1 > 0.2$ , and amount of trapped charge reaches a plateau at  $a_1 > 1$  [14]. As the charge increases we observe a decrease in energy gain and increase of energy spread and emittance due to beam loading. Energy spread could be controlled by lengthening the bunch length, and locking the bunch phase by using plasma density tapering [15]. The energy gain could also be controlled by varying the bunch injection phase in the wake by using a three pulse scheme.

Note that even though all parameter scans were performed with 2D PIC simulations, we verified that the physics is robust by performing 3D benchmark. 3D simulations suggest that the energy gain can be 20% less because of stronger beam loading; however, the beam charge, emittance and energy spread are well represented in the 2D geometry.

## LASER EVOLUTION AND HIGHER ORDER MODES

Even though introducing a plasma channel allows for higher energy gain of the electron beam, its depth must be adjusted carefully so the main laser pulse does not over focus and undergo betatron oscillations. For a low intensity laser the matched condition for the plasma channel is

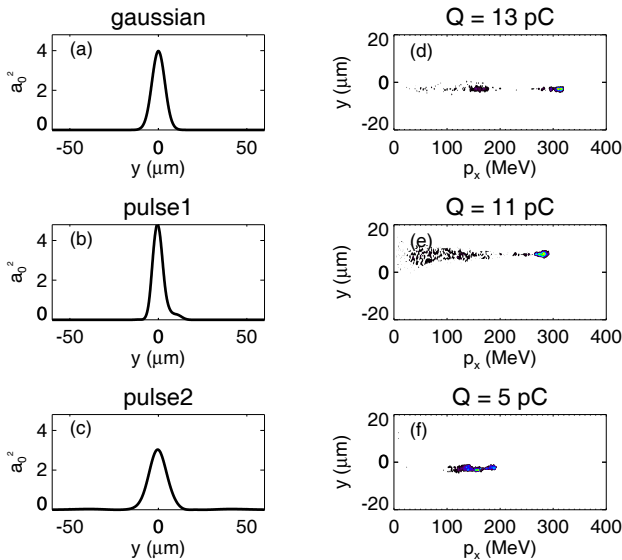


Figure 4: Transverse laser profile is shown for (a) the ideal Gaussian mode, and (b), (c) combination of Hermite-Gaussian modes up to third order. The corresponding electron beam profile at dephasing is shown in (d) - (f).

for its transverse profile to be of the form  $n(r) = n_0 + \Delta n_c (r/w_m)^2$ , with  $\Delta n_c [\text{cm}^{-3}] = 1.13 \times 10^{20}/w_m^2 [\mu\text{m}]$ , and where  $w_m$  is the matched spot of the channel and is equal to the laser spot size,  $w_m = w_0$ . For a higher intensity laser, as power gets close to the critical power,  $P_c = 17 (\lambda_p/\lambda)^2 \text{ GW}$ , we must choose  $w_m > w_0$  to compensate for self-focusing. Self-focusing of the driver right after interaction of the two laser pulses where the electron beam is trapped can lead to decrease of the trapped charge in the bunch. This happens as the bubble length reduces when the laser spot size decreases. Some of the particles, originally trapped in the bubble are then located in a defocusing phase, and are lost from the trapped bunch. Simulations show that as the channel gets wider, more charge stays in the bunch, because the laser self-focuses less and more slowly. We find that a channel with  $w_m = 9 \mu\text{m}$  matches well the laser, avoiding betatron oscillations, and keeping all the charge in the beam, while still retaining guiding necessary for high energy beam.

While simulations are often performed with perfect Gaussian modes for the laser pulse, some higher order mode content can exist in high power lasers used to drive experiments. We evaluate the effects of such higher order mode content with 2D simulations by fitting laser pulse profiles recorded in the experiment with Hermite-Gaussian modes up to third order. Different transverse laser profiles used in the simulation are shown in Fig. 4. Figure 4 (a) shows the perfect Gaussian mode as reference, and Fig. 4 (b) and (c) show two laser profiles with higher order mode content. Figure 4 (d)–(f) show the corresponding electron bunch profile at dephasing. While the electron beam is slightly steered off axis with the perfect Gaussian mode

( $y \simeq -2.6 \mu\text{m}$ ) [Fig. 4 (d)], we observed that this can be corrected by adjusting the timing between the two colliding pulses. The presence of an asymmetric side lobe [Fig. 4 (b)] leads to steering of the electron beam off axis ( $y \simeq 8 \mu\text{m}$ ) as the laser peak intensity evolves towards positive  $y$  with propagation distance. Reduction of the intensity of the main peak [Fig. 4 (c)] leads to less trapped charge, as the product  $a_0 a_1$  is decreased, and significant degradation of the quality of the bunch. This shows that it is important to control the quality of the main laser pulse to obtain high quality electron bunches. This is performed in the lab by using deformable mirrors.

## CONCLUSION

Self-consistent PIC simulations performed with the VORPAL framework, were used to predict and design colliding laser pulse injection experiments at LBNL. Simulations have shown that for the parameters accessible in these experiments high quality, 20 pC, electron bunch can be accelerated to 300 MeV with few percent energy spread and emittance of the order of 2 mm mrad. First experimental results have shown good agreement with simulation data, which gives confidence in the ability of the simulations to predict the outcome of the experiments. Parameter scans show that the properties of the beam can be controlled independently by changing either the plasma density or the laser parameters. We have also stressed the importance of controlling the plasma channel and the mode of the main laser pulse to guarantee the quality of the final electron bunch. Further beam optimization and control can be achieved by using a CPI scheme with three laser pulses, where two lasers of lower intensity collide behind the driver pulse. This will be the object of future study both with simulations and experiments.

## REFERENCES

- [1] E. Esarey *et al.*, Rev. Mod. Phys., 81, (2009), 1229.
- [2] S.P.D. Mangles *et al.*, C.G.R. Geddes *et al.*, J. Faure *et al.*, Nature, 431, (2004), 535 – 544.
- [3] W.P. Leemans *et al.*, Nature Phys., 2, (2006), 696 – 699.
- [4] C.B. Schroeder *et al.*, AIP Conf. Proc., 1086, (2009), 208.
- [5] C.G.R. Geddes *et al.*, AIP Conf. Proc., 1099, (2009), 666.
- [6] C.G.R. Geddes *et al.*, Phys. Rev. Lett., 100, (2008), 215004.
- [7] A. Pak *et al.*, C. McGuffey *et al.*, Phys. Rev. Lett., 104, (2010), 025003 – 025004.
- [8] E. Esarey *et al.*, Phys. Rev. Lett., 79, (1997), 2682.
- [9] C.B. Schroeder *et al.*, Phys. Rev. E., 59, (1999), 6037.
- [10] G. Fubiani *et al.*, Phys. Rev. E., 70, (2004), 016402.
- [11] J.R. Cary *et al.*, Phys. Plasmas, 12, (2005), 056704.
- [12] J. Faure *et al.*, Nature, 444, (2006), 737.
- [13] C. Nieter *et al.*, J. Compt. Phys., 196, (2004), 448.
- [14] C.G.R. Geddes *et al.*, these proceedings.
- [15] E. Cormier-Michel *et al.*, AIP Conf. Proc., 1086, (2009), 297.